



Universiteit
Leiden
The Netherlands

Disconnected self: influence of dissociation on emotional distractibility in Borderline Personality Disorder: a neuroimaging approach

Krause, A.D.

Citation

Krause, A. D. (2017, November 16). *Disconnected self: influence of dissociation on emotional distractibility in Borderline Personality Disorder: a neuroimaging approach*. Retrieved from <https://hdl.handle.net/1887/60261>

Version: Publisher's Version

License: [Licence agreement concerning inclusion of doctoral thesis in the Institutional Repository of the University of Leiden](#)

Downloaded from: <https://hdl.handle.net/1887/60261>

Note: To cite this publication please use the final published version (if applicable).

Cover Page



Universiteit Leiden



The handle <http://hdl.handle.net/1887/60261> holds various files of this Leiden University dissertation.

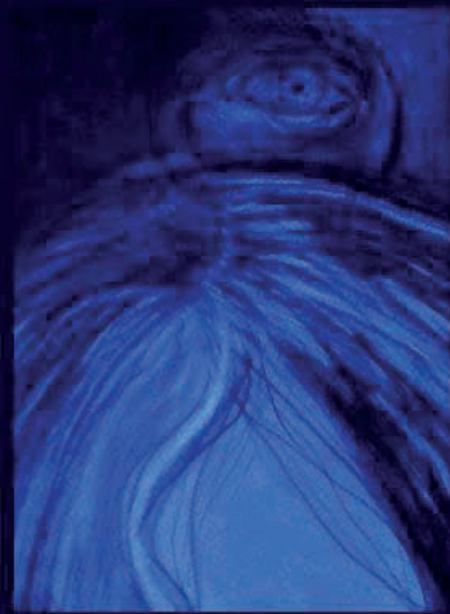
Author: Krause, A.D.

Title: Disconnected self: influence of dissociation on emotional distractibility in Borderline Personality Disorder: a neuroimaging approach

Issue Date: 2017-11-16

Chapter 4 – 7

Neuroimaging studies



CHAPTER 4

Amygdala and Anterior Cingulate Resting-state Functional Connectivity in Borderline Personality Disorder – Associations with Trait Dissociation

Annegret Krause-Utz*, Ilya M. Veer*, Serge A. R. B. Rombouts, Martin Bohus, Christian Schmahl, and Bernet M. Elzinga (2014c). Amygdala and anterior cingulate resting-state functional connectivity in borderline personality disorder patients with a history of interpersonal trauma. *Psychological Medicine*, 44(13), 2889-2901. *contributed equally

Abstract

Background: Studies in Borderline Personality Disorder (BPD) have consistently revealed abnormalities in fronto-limbic brain regions during emotional, somatosensory, and cognitive challenges. Here we investigated changes in resting-state functional connectivity (RSFC) of three fronto-limbic core regions of specific importance to BPD. **Methods:** Functional magnetic resonance imaging data was acquired in 20 unmedicated female BPD patients and 17 healthy controls (HC, matched for age, sex, and education) during rest. The amygdala, dorsal and ventral anterior cingulate cortex (ACC) were defined as seeds to investigate RSFC patterns of a medial temporal lobe network, the salience network, and default mode network. The Dissociation Experience Scale (DES), a measure of trait dissociation, was additionally used as predictor of RSFC with these seed regions. **Results:** Compared to HC, BPD patients showed a trend towards increased RSFC between the amygdala and the insula, orbitofrontal cortex, and putamen. Compared to controls, patients furthermore exhibited diminished negative RSFC between the dorsal ACC and posterior cingulate cortex, a core region of the default mode network, and regions of the dorsomedial prefrontal cortex. Lastly, increased negative RSFC between the ventral ACC and medial occipital regions was observed in BPD patients. DES scores were correlated with amygdala connectivity with the dorsolateral prefrontal cortex and fusiform gyrus. **Conclusions:** Our findings suggest alterations in resting-state networks associated with processing of negative emotions, encoding of salient events, and self-referential processing in individuals with BPD compared to HC. These results shed more light on the role of brain connectivity in the pathophysiology of BPD.

Key words: Borderline Personality Disorder, resting-state fMRI, functional connectivity, amygdala, anterior cingulate cortex, dissociation

4.1. Introduction

Borderline Personality Disorder (BPD) is a severe mental disorder characterized by pronounced difficulties in emotion regulation, interpersonal disturbances (e.g., frantic efforts to avoid abandonment), negative self-concept, and stress-related dissociation (APA, 2000; Skodol et al., 2002; Leichsenring et al., 2011). During emotional and somatosensory challenge, individuals with BPD have shown alterations within a network of fronto-limbic brain regions that might underlie key features of this disorder (see Leichsenring et al., 2011; O'Neill & Frodl, 2012).

Functional magnetic resonance imaging (fMRI) studies of BPD consistently have shown amygdala hyperactivity during exposure to emotionally arousing pictures and fearful faces compared to healthy participants (see Leichsenring et al., 2011; O'Neill & Frodl, 2012). Given the critical role of the amygdala in emotion processing (Davis & Whalen, 2001; Phillips et al., 2003; Phan et al., 2004; Ochsner & Gross, 2007), hyperactivity of this area may underlie clinically well-observed BPD features such as emotional hypersensitivity and intense, long-lasting emotional reactions (Leichsenring et al., 2011). Yet, contradictory results have also been reported (Ruocco et al., 2013), in accordance with findings from behavioral studies in BPD: Whereas some studies revealed enhanced emotion detection, others showed emotion detection to be reduced in BPD (Lis & Bohus, 2013). Specific states may in fact modulate emotion processing and amygdala activation in BPD. For example, it has been proposed that limbic activation is dampened during states of dissociation (Sierra & Berrios, 1998; Lanius et al., 2010), a core feature of BPD (APA, 2000). Moreover, some studies in BPD found amygdala hyperactivity to normative neutral pictures (Donegan et al., 2003; Koenigsberg et al., 2009a; Niedtfeld et al., 2010; Schulze et al., 2011; Krause-Utz et al., 2012), possibly due to a tendency to interpret normative neutral stimuli as emotionally arousing, which may result in increased states of vigilance in BPD (Lis & Bohus, 2013).

Aside from limbic alterations, BPD patients have shown abnormal recruitment of frontal brain regions that are typically involved in top-down emotion regulation (Phillips et al., 2003; Ochsner & Gross, 2007; Etkin et al., 2011; Banks et al., 2007) and impulse control (Pessoa et al., 2012): For example, BPD patients exhibited diminished recruitment of frontal brain regions including the anterior cingulate cortex (ACC), dorsomedial prefrontal cortex (dmPFC), dorsolateral prefrontal cortex (DLPFC), and orbitofrontal cortex (OFC), while being instructed to inhibit emotional processing (Schulze et al., 2011; Koenigsberg et al., 2009b; Lang et al., 2012) and during cognitive inhibition tasks (Silbersweig et al., 2007). Moreover, BPD patients activated the ACC less than controls during exposure to fearful faces (Minzenberg et al., 2007) and trauma-related scripts (Schmahl et al., 2003, 2004).

Over the last decade, studying how brain regions interact in absence of goal directed behavior (resting-state functional connectivity; RSFC) has become increasingly important in understanding the neurobiology of psychiatric disorders (Greicius, 2008). Yet to date only two studies have investigated this in BPD (Wolf et al., 2011; Doll et al., 2013). Wolf and colleagues revealed altered connectivity within the default mode network, which has been related to pain processing and self-referential processes such as episodic memory and self-monitoring (Raichle et al., 2001; Greicius et al., 2003; Menon, 2011): Compared to healthy participants, BPD patients showed increased RSFC in the left frontal pole and left insula as well as decreased RSFC in the left cuneus. BPD patients further exhibited decreased RSFC in the left inferior parietal lobule and right middle temporal cortex within a network comprising fronto-parietal brain areas (task-positive network) compared to healthy individuals. Interestingly, RSFC of the insula and cuneus was positively correlated with self-reported dissociation (Wolf et al., 2011). Doll and colleagues (2013) reported altered RSFC in the default mode and task-positive networks, in line with the findings of Wolf and colleagues (2011). Moreover, BPD patients showed aberrant RSFC in the salience network, comprising the orbitofrontal insula and dorsal ACC (dACC). This network has been associated with interoceptive awareness, detection of salient events, encoding of unpleasant feelings, and a wide variety of cognitive tasks (Seeley et al., 2007; Menon & Uddin, 2010). Doll and colleagues (2013) further showed imbalanced connections between the three networks, most prominently a shift from RSFC in the task-positive to increased RSFC in the salience network in BPD patients. However, a drawback of both studies was that most patients were on psychotropic medication.

Here, we investigate RSFC patterns in unmedicated individuals with BPD compared to age- and education-matched healthy controls (HC), using three seed regions of interest that are of particular relevance to BPD psychopathology based on current neurobiological models of the disorder and previous neuroimaging research (see Leichsenring et al., 2011). Each of these seed regions has been found to probe a specific intrinsic connectivity network: 1) bilateral amygdala (*medial temporal lobe network*), 2) dACC (*salience network*), and 3) ventral ACC (vACC) (*default mode network*). Based on previous research, we expected altered RSFC between our seeds and brain regions mainly located in the vm/dmPFC, insula, and occipital cortex in BPD patients. In addition, an exploratory analysis was carried out in the BPD group to assess the relation between trait dissociation and RSFC of the three seeds.

4.2. Methods and Materials

4.2.1. Participants

Thirty-nine females between 18 and 45 participated in this study. Two patients were excluded, because they reported to have fallen asleep during scanning. All participants underwent diagnostic assessments including the Structured Interview for DSM-IV Axis-I (SCID-I) (First et al., 1997) and the International Personality Disorder Examination (IPDE) (Loranger et al., 1999) by trained diagnosticians (inter-rater reliability: $\kappa=.77$ for all interviews). Clinical assessment included questionnaires on BPD symptom severity (BSL-95, Bohus et al., 2007), Posttraumatic Stress Disorder (PTSD) symptoms and childhood trauma history (PDS, Foa, 1995; CTQ, Bernstein et al., 2003), trait dissociation (DES, Bernstein & Putnam, 1986), dysphoric mood (BDI, Beck et al. 1961), impulsivity (BIS-10, Patton et al. 1995), difficulties in emotion regulation (DERS, Gratz & Roemer, 2004), affect intensity (AIM, Larsen, 1984), and current self-injurious behavior. General MRI exclusion criteria were: metal implants, pregnancy, and left-handedness. BPD patients were free of medication within the last 14 days (in case of fluoxetine 28 days), free of severe somatic illness, and free of substance dependence within the last 6 months. Further exclusion criteria for the patient group were: current major depression, lifetime diagnoses of psychotic disorder, bipolar affective disorder, mental retardation, developmental disorder, and life-threatening suicidal crisis. Exclusion criteria for the HC group were: lifetime diagnoses of psychiatric and somatic disorders. The final patient group comprised 20 unmedicated females meeting criteria for BPD according to DSM-IV (APA, 2000). All patients fulfilled DSM-IV criterion 6 for emotional instability and reported a history of physical, sexual, and/or emotional trauma as assessed by the PDS and CTQ. Clinical characteristics and co-occurring mental conditions in the patient sample are reported in Table 4.1. In our BPD sample, nine patients met criteria for current comorbid PTSD. The final HC group comprised 17 participants without a history of psychiatric disorders and trauma. The groups did not differ regarding age, education level, and body mass index (BMI) (Table 4.1).

4.2.2. Procedure

The experiment was approved by the local medical ethics committee (University of Heidelberg, in accordance to the World Medical Association's Declaration of Helsinki) and conducted at the Central Institute of Mental Health in Mannheim, Germany. All participants were informed about the experiment and scanning procedure. Written informed consent was obtained. Before scanning, participants underwent diagnostic interviews (SCID-I, IPDE) and completed the questionnaires. Acquisition of RS was positioned first in the scanning protocol.

Participants were instructed to lie still with their eyes closed and not to fall asleep during this scan. Compliance to these instructions was verified as part of the exit interview. After the resting-state scan several anatomical and functional scans were acquired (Krause-Utz et al., 2012). After scanning, participants were debriefed, thanked, and paid for participation.

Table 4.1.

Demographic and clinical variables in healthy participants (HC) and patients with Borderline Personality Disorder (BPD)

	BPD (N=20)	HC (N=17)	t-tests (df=35)
Age	29.55 ± 7.74	27.53 ± 8.58	$t=0.75, p=.456$
Weight	70.32 ± 21.23	63.88 ± 13.32	$t=1.08, p=.289$
BMI	25.24 ± 6.92	23.29 ± 4.17	$t=1.00, p=.324$
Education level			
9 years secondary school	N=2 (10%)	N=1 (6%)	$\chi^2=3.25, p=.197$
10 year secondary school	N=7 (35%)	N=2 (12%)	
13 year secondary school	N=11 (55%)	N=14 (82%)	
BSL-95 (total score)	188.88 ± 52.40	24.10 ± 12.93	$t=13.38, p<.0001$
CTQ (total score)	47.38 ± 19.93	20.55 ± 5.41	$t=4.49, p<.0001$
DES (total score)	32.25 ± 15.78	2.21 ± 1.69	$t=8.45, p<.0001$
AIM (total score)	50.07 ± 13.68		
BDI (total score)	22.67 ± 10.64		
BIS (total score)	88.82 ± 10.37		
DERS (total score)	87.93 ± 25.76		
Self-injurious behavior	N=9 (45%)		
PTSD current/lifetime	N=9 (45%)		
Past major depression	N=8 (40%)		
Social phobia lifetime	N=2 (10%)		
Panic disorder lifetime	N=2 (10%)		
Specific phobia lifetime	N=1 (5%)		
Past substance abuse	N=4 (20%)		
Eating disorder lifetime	N=7 (35%)		

Note: BSL-95 = Borderline Symptom List 95; CTQ = Childhood Trauma Questionnaire; DES = Dissociation Experience Scale; AIM = Affect Intensity Measure; BDI = Beck Depression Inventory; BIS = Barratt Impulsiveness Scale; DERS = Difficulties in Emotion Regulation Scale; PTSD = Posttraumatic Stress Disorder

4.2.3. FMRI data acquisition and analysis

MRI scans were acquired on a Siemens TRIO-3T MRI scanner using an eight-channel head coil (Siemens Medical Solutions, Germany). Whole-brain resting-state scans were acquired using T_2^* -weighted gradient-echo echo-planar imaging (EPI, 150 volumes, 40 sagittal slices scanned in ascending order, repetition time (TR) 2500ms, echo time (TE) 30ms, flip angle 80° , field of view 220x220mm, 3mm isotropic voxels with no slice gap). A high-resolution 3D T_1 -weighted anatomical image (MPRAGE, 1mm isotropic voxels) was acquired for registration purposes. Head movement artifacts and scanning noise were restricted using head cushions and headphones within the scanner coil.

4.2.3.1. FMRI data preprocessing

Prior to analysis, all RS-fMRI data sets underwent a visual quality control check to ensure that no gross artifacts were present in the data. Afterwards, data were analyzed using FSL Version 4.1.7 (FMRIB's Software Library, www.fmrib.ox.ac.uk/fsl) (Smith et al., 2004). The following preprocessing steps were applied to EPI data sets: motion correction (Jenkinson et al., 2002), removal of non-brain tissue (Smith et al., 2004), spatial smoothing using a Gaussian kernel of 6mm full width at half maximum (FWHM), grand-mean intensity normalization of the entire 4D dataset by a single multiplicative factor, a high-pass temporal filter of 100 seconds (i.e., $\geq 0.01\text{Hz}$). The RS-fMRI dataset was registered to the T_1 -weighted image, and the T_1 -weighted image to the 2mm isotropic Montreal Neurological Institute (MNI) standard space image (T_1 -weighted standard brain averaged over 152 subjects (MNI-152), Montreal, QC, Canada) (Jenkinson et al., 2002; Jenkinson & Smith, 2001). The resulting transformation matrices were combined to obtain a native to MNI space transformation matrix.

4.2.3.2. FMRI time course extraction and statistical analysis

A seed-based correlation analysis (Fox & Raichle, 2007) was employed to reveal brain areas that are functionally connected to a-priori defined seed regions of interest (ROI) during rest. The amygdala (*medial temporal lobe network*; MNI coordinates $X=\pm 23$, $Y=-4$, $Z=-19$; Veer, Oei, Spinhoven, van Buchem, Elzinga, & Rombouts, 2011) was defined as first seed region. The second seed region was the dACC (*salience network*; MNI coordinates $X=\pm 5$, $Y=19$, $Z=28$, seed "14" in Margulies, Kelly, Uddin, Biswal, Castellanos, & Milham, 2007). The third seed region was the vACC (*default mode network*; MNI coordinates $X=\pm 5$, $Y=47$, $Z=11$, seed "S7" in Margulies et al., 2007). Spherical regions of interest were created around these voxels using a radius of 4mm. Next, all masks were registered to each participant's RS-fMRI preprocessed dataset using the inverse transformation matrix. The mean time courses were subsequently extracted from the voxels falling within each mask in native space.

The time courses of the left and right seeds were entered as a regressor in a general linear model (GLM), for each of the three networks separately, together with nine nuisance regressors comprising the white matter signal, CSF signal, six motion parameters (three translations and three rotations) and the global signal. The latter regressor was included to further reduce the influence of artifacts caused by physiological signal sources (i.e., cardiac and respiratory) on the results (Fox & Raichle, 2007). However, because regression of the global signal can induce either anti-correlations or even group differences (Murphy et al., 2009; Saad et al., 2012), we repeated all analysis without the global signal as regressor in the model. Each individual model was tested using FEAT version 5.98, part of FSL, with contrasts for left and right seeds separately, as well as a contrast to assess FC of the left and right seeds together. The resulting individual parameter estimate maps, together with their corresponding within-subject variance maps, were then resliced into 2 mm isotropic MNI space and fed into a higher level mixed effects regression analysis and compared between groups (independent-samples t-test). Post-hoc correlations were carried out between symptom severity scores (BSL-95) and brain regions showing significant between-group differences. In addition, an exploratory whole-brain analysis was conducted for the BPD group to investigate the relation between trait dissociation scores (DES) and RSFC with each of the three seeds. To this end, a higher-level mixed effects regression analysis was carried out including DES scores as regressor of interest, for each of the three networks separately. All statistical images were whole-brain corrected for multiple comparisons using cluster-based thresholding with an initial cluster-forming threshold of $Z > 2.3$ and a corrected cluster significance threshold of $p < 0.017$ ($p < .05$, Bonferroni corrected for the 3 networks tested; Worsley, 2001). Based on our a-priori hypothesis on altered amygdala-mPFC connectivity, a small volume correction was applied for mPFC regions, including the pgACC, vm/dmPFC and OFC. A combined mask of these ROIs was created based on the Harvard–Oxford cortical probability atlas, as provided in FSL, which was then used to mask the raw statistical images. Subsequently, correction for multiple comparisons was carried out for those voxels present in the mask (mPFC) using cluster based thresholding with the same parameter settings as for the whole-brain analysis ($Z > 2.3$, $p < .017$).

Since nine BPD patients additionally met criteria for PTSD, we ran an additional post-hoc analysis to assess the effects of comorbidity on functional connectivity (details from this analysis can be found in the Supplemental Methods).

4.3. Results

4.3.1. Amygdala connectivity (medial temporal lobe network)

Overall, amygdala RSFC in both groups was highly similar to the patterns previously described in literature (Roy et al., 2009; Veer et al., 2011) (Supplemental Fig. 4.1A). At our stringent threshold of $p < .017$, no differences were observed between the two groups. However, a trend was observed for a cluster comprising the lateral OFC, putamen and dorsal insula ($p < .05$, whole brain corrected; Figure 4.1A): While HC showed no RSFC between the right amygdala and this cluster, this positive functional connection was present in BPD patients (see Table 4.2). Our ROI analysis of amygdala-mPFC RSFC did not yield any differences between the two groups.

Table 4.2.

Resting-state functional connectivity results: Between groups effects

Region	Cluster size 2mm voxels	Peak voxel coordinates (MNI)			Z-value
		x	y	z	
<u>Amygdala seed</u>					
BPD>HC					
Insula	331	34	4	8	3.68 *
Orbitofrontal cortex		32	12	-22	3.22 *
Putamen		20	8	-4	2.99 *
<u>Dorsal ACC seed (I4)</u>					
BPD>HC					
Rostral anterior paracingulate cortex	773	8	50	14	3.8
HC>BPD					
Posterior cingulate cortex	521	-2	-56	20	4.17
<u>Ventral ACC seed (S7)</u>					
BPD>HC					
Medial visual cortex	709	-6	-90	10	3.7

Note: all z-values are cluster corrected for multiple comparisons ($p < .017$), except for z-values with a * ($p < .05$).

4.3.2. Dorsal ACC connectivity (salience network)

In both patients and controls the pattern of brain regions comprising the salience network (see Supplemental Fig. 4.1B) overlapped with connectivity patterns found in previous studies (Seeley et al., 2007; Menon & Uddin, 2010). Figure 4.1B illustrates regions in which group differences in bilateral dACC RSFC were observed between BPD patients and HC (also see Table 4.2): While HC showed strong negative RSFC between bilateral dACC and left PCC, decreased negative RSFC between these regions was found in BPD patients. Additionally, increased dACC RSFC with two clusters in the dorsomedial PFC/paracingulate cortex was found in BPD patients compared to HC. In BPD patients, both clusters were positively correlated with the dACC. In HC, the lower cluster showed negative connectivity and the upper cluster showed diminished connectivity with the dACC (see Table 4.2).

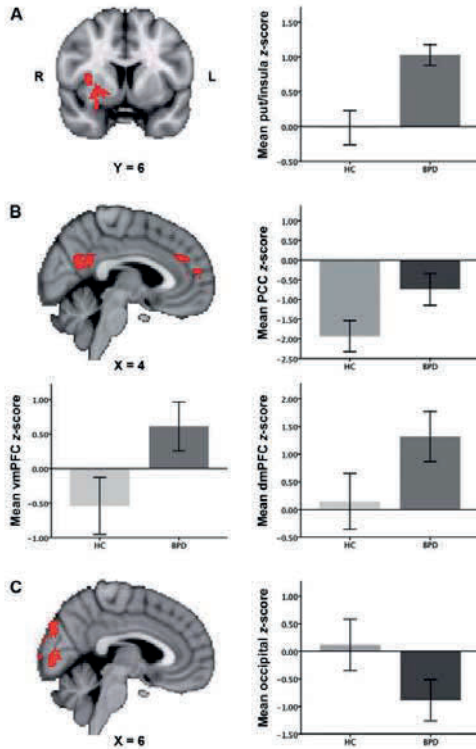


Figure 4.1. Between-group differences in resting-state functional connectivity of each of the three seeds: A) Amygdala (medial temporal lobe network); B) Dorsal ACC (salience network); C) Ventral ACC (default mode network). Connectivity differences are overlaid on the MNI 2mm standard space template. Bar graphs plot the mean Z-scores (± 2 standard errors of the mean) in each group for each of the regions where connectivity differences are found ($Z > 2.3$, $p < .017$; whole brain cluster corrected, except for Figure 4.1A: $Z > 2.3$, $p < .05$).

4.3.3. Ventral ACC connectivity (default mode network)

Both groups demonstrated vACC connectivity with well-described areas of the default mode network including the PCC, precuneus, and lateral parietal cortex (Raichle et al., 2001; Greicius et al., 2003; Menon, 2011) (see Supplemental Fig. 4.1C). Patients showed increased negative RSFC between left vACC and area V1 of the occipital cortex, lingual gyrus, and cuneus compared to HC who exhibited marginal RSFC with these regions (Fig. 4.1C, Table 4.2). In the patient group, there were no significant correlations between BPD symptom severity scores (BSL-95) and the FC strength of any of the brain regions in which between-group differences were found.

4.3.4. Exploratory analysis: Trait dissociation and functional connectivity

In BPD, correlations were found between DES-scores and amygdala RSFC with several brain regions. First, a positive correlation with left amygdala-right dlPFC RSFC was observed (Fig. 4.2A, Table 4.3), illustrating stronger RSFC between these regions in patients with higher self-reported trait dissociation. Secondly, DES scores differentially modulated left amygdala RSFC with a cluster in the occipital lobe including the lingual gyrus, intracalcarine cortex, and fusiform gyrus (Fig 4.2B, Table 4.3), demonstrating increasing negative RSFC between these regions with higher DES scores. Correlations for bilateral amygdala RSFC were similar to those for left amygdala. No associations were found with RSFC of the other seeds.

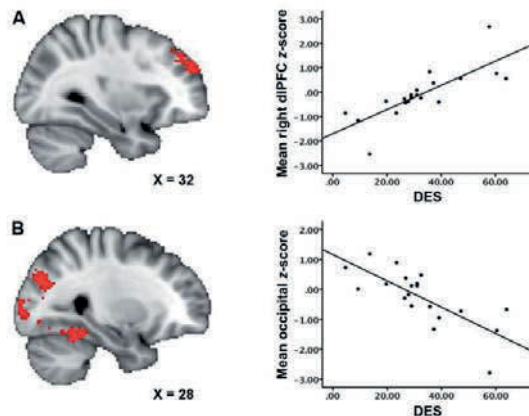


Figure 4.2. Voxel-wise correlations between trait dissociation scores (DES) and amygdala RSFC in BPD ($Z > 2.3$, $p < .017$; whole brain cluster corrected): A) Left amygdala-dlPFC connectivity is positively associated with trait dissociation; B) Left amygdala-occipital cortex connectivity (including the lingual gyrus, intracalcarine cortex, and fusiform gyrus) is negatively associated with trait dissociation. Results are overlaid on the MNI 2mm standard space template, according to the radiological convention. Scatter plots illustrate the direction of the correlation, with mean Z-scores plotted against the dissociation scores.

Table 4.3.

DES associations with amygdala resting-state functional connectivity in the BPD group

Region	Hemisphere	Cluster size 2mm voxels	Peak voxel coordinates (MNI)			Z-value
			X	y	Z	
Positive association Dorsolateral prefrontal cortex	R	643	40	38	38	3.76
Negative association Lingual gyrus	R	3361	12	-64	-10	4.28
Lateral occipital cortex	R		44	-84	-6	4.05
Fusiform gyrus	R		36	-58	-20	4.00
Intracalcarine cortex	R		4	-86	4	3.93

4.3.5. Effects of global signal regression

Reanalysis without the global signal revealed highly similar results. Although some of the effects did not survive the stringent multiple comparison correction, these could still be observed at a more lenient threshold (see Supplemental Figures S4.2 and S4.3, and Supplemental Tables S4.1 and S4.2).

4.3.6. Subgroup analysis

No differences were found between BPD with or without comorbid PTSD. Full results of this analysis are reported the Supplemental Material.

4.4. Discussion

Here we investigated resting-state functional connectivity in unmedicated Borderline Personality Disorder (BPD) patients compared to healthy controls (HC). Three seeds of high relevance to BPD psychopathology were chosen, each probing a specific brain network: 1) bilateral amygdala (*medial temporal lobe network*), 2) dACC (*saliency network*), and 3) vACC (*default mode network*). In both groups, we could replicate connectivity patterns reported in previous studies (Margulies et al., 2007; Veer et al., 2011). Overall, RSFC differences between BPD patients and controls were observed within networks associated with the processing of negative emotions, encoding of salient events, and self-referential processing. The results per seed are discussed in more detail below.

Amygdala connectivity (medial temporal lobe network)

The amygdala plays a key role in emotion processing and the initiation of fear and stress responses (Davis & Whalen, 2001; Phillips et al., 2003; Ochsner & Gross, 2007), and has functional connections with the perigenual ACC, insula, and OFC (Stein et al., 2007).

The insula and OFC have been implicated in identifying the emotional significance of internal and external stimuli and the generation of emotional responses (Phillips et al., 2003; Banks et al., 2007; Kringelbach & Rolls, 2004; Ochsner & Gross, 2007; Etkin et al., 2011). Several studies in BPD patients reported hyperactivity of the amygdala and insula during emotional challenge (Niedtfeld et al., 2010; Schulze et al., 2011; Leichsenring et al., 2011; Krause-Utz et al., 2012; O'Neill & Frodl, 2012). In the present study, we found a stronger coupling between the amygdala and a cluster comprising the dorsal insula, OFC, and putamen in BPD patients than in HC even in the absence of experimental conditions. Since this effect did not pass a more stringent correction for testing multiple seeds, it has to be discussed as a trend effect and therefore treated with caution. Nevertheless, in the context of earlier studies, our trend finding of amygdala hyper-connectivity with other brain regions highly relevant to emotion processing, could reflect the clinically well-observed BPD feature of affective hyperarousal and intense emotional reactions. Indeed, high levels of aversive affective arousal, often accompanied by dissociative experiences, are a major characteristic of BPD (Linehan, 1993; Stiglmayr et al., 2001; Stiglmayr et al., 2008). Affective hyperarousal often leads to self-inflicted harm, suicidal acts and dysfunctional impulsive behavior patterns, therefore having detrimental consequences in patients with BPD (Chapman, Gratz, & Brown, 2006; Kemperman, Russ, & Shearin, 1997; Kleindienst et al., 2008). In addition, we observed a stronger coupling between the amygdala and putamen in BPD patients than in controls. Being part of the basal ganglia, the putamen is involved in movement control (Packard & Knowlton, 2002) and may play an important role in mobilizing an individual to take action in the face of contempt and disgust (Zeki et al., 2008). Furthermore, both the OFC and the putamen play an important role in reward processing, reinforcement learning, and impulsivity (Packard & Knowlton, 2002; Kringelbach & Rolls, 2004; Haber & Knutson, 2010), which is another key feature of BPD.

ACC connectivity (salience network, default mode network)

Being an important constituent of the salience network, the dACC has been related to the detection of salient events and a wide variety of cognitively demanding tasks (Menon & Uddin, 2010; Critchley et al., 2001; Dosenbach et al., 2006; Sridharan et al., 2008). Moreover, recent studies have highlighted the role of the dACC and orbitofrontal insula in switching between different large-scale networks and reallocating cognitive resources in the face of salient events.

Across different samples of healthy participants, Sridharan and colleagues (2008) demonstrated that activation in the dACC temporally precedes activity in nodes of other networks such as the PCC. In other studies, healthy individuals recurrently showed strong anti-correlations between ‘task-positive’ brain regions (e.g., dACC) and regions commonly activated during rest (e.g., PCC) (Fox et al., 2005; Buckner & Vincent, 2007; Neumann et al., 2010).

Notably, in the present study, healthy controls showed a negative association between the dACC and PCC compared to BPD patients who exhibited diminished anti-correlations between these regions. Moreover, BPD patients showed a stronger RSFC of our seed with the dorsomedial PFC, whereas healthy participants showed diminished connectivity between these regions. The dorsomedial PFC has been critically implicated in self-referential processes such as processing of autobiographical memories and monitoring of internal cognitive and affective states (Buckner & Vincent, 2007).

Our findings of diminished interaction between core regions of the salience and default mode networks could suggest impaired flexibility in switching between the networks. Similarly, a recent RS-fMRI study in BPD patients reported imbalanced inter-network connectivity between the default mode network and the salience network (Doll et al., 2013). Although the nature of these interactions between brain networks is not yet fully understood, our findings might translate into an increased vigilance even to seemingly neutral events in individuals with BPD (Kluetsch et al., 2012; Lis & Bohus, 2013).

BPD patients further showed decreased RSFC between left vACC and area V1 of the occipital cortex, lingual gyrus, and cuneus compared to controls, which showed only marginal RSFC between these regions. In part, these findings are in line with previous fMRI studies in BPD who reported altered RSFC within the default mode network in BPD (Wolf et al., 2011; Doll et al., 2013). More specific, Wolf and colleagues (2011) observed altered RSFC in the left cuneus as well as in the insula and frontopolar cortex in BPD patients compared to HC. Diminished RSFC in occipital areas within the default mode network may be associated with an inflexible integration of sensory stimuli into self-referential processing in individuals with BPD (Wolf et al., 2011). In the previous RS-fMRI study by Wolf and colleagues (2011), altered cuneus RSFC within the default mode network was negatively correlated with self-reported dissociative states in patients with BPD.

Trait dissociation and functional connectivity

Our exploratory analysis revealed negative correlations between self-reported trait dissociation and amygdala RSFC with the cuneus, area V1 of the occipital lobe, and the fusiform gyrus in BPD patients, partly in line with findings by Wolf and colleagues (2011).

Diminished amygdala RSFC in occipital areas may represent an altered gating of sensory input associated with self-reported dissociation (Lanius et al., 2005).

Wolf and colleagues further found positive correlations between self-reported dissociative states and insula RSFC, which were not observed in the present study. Instead, we revealed positive correlations between self-reported dissociation and left amygdala RSFC in the right dlPFC – a brain area involved in working memory, attention deployment, and inhibitory control of emotions (Ochsner & Gross, 2007). It has been proposed that dissociation is associated with increased prefrontal inhibition of limbic brain activation, which reflects an over-modulation of emotional arousal (Lanius et al., 2010). Indeed, states of dissociation negatively predicted amygdala activation during emotional interference in BPD patients with a history of trauma (Krause-Utz et al., 2012). Further neuroimaging studies are needed to gain more insight into the neurobiological underpinnings of this complex phenomenon.

Several limitations need to be addressed: First, since all of our patients reported a history of interpersonal trauma – which is highly prevalent in BPD (APA, 2000; Leichsenring et al., 2011) – our findings could also be related to the history of interpersonal trauma in general, rather than to BPD psychopathology in particular. However, although a recent study in participants with a history of childhood maltreatment demonstrated abnormal amygdala RSFC with the putamen and insula (van der Werff et al., 2012), this connection was decreased rather than increased. Further, the presence of comorbid conditions limits the specificity of our results as well, even though most individuals with BPD have additional axis I disorders (Leichsenring et al., 2011). More specific, nine patients in the present BPD sample additionally met criteria for PTSD. As aberrant amygdala (Sripada et al., 2012; Rabinak et al., 2011) and default mode (Lanius et al., 2010; Daniels et al., 2010) RSFC has been observed in PTSD patients previously, a post-hoc comparison between BPD patients with or without comorbid PTSD was carried out. This revealed no significant differences between subgroups, while BPD patients with and without comorbid PTSD all differed significantly from HC in each cluster found in the main analysis but one. In addition, DES scores predicted amygdala connectivity with the DLPFC and occipital cortex to the same extent in both BPD subgroups. These results suggest that group differences found in our study cannot be explained merely by the presence of comorbid PTSD. Nevertheless, future studies have to compare BPD patients to patients with other disorders (e.g., PTSD) to clarify whether the alterations in RSFC described here are truly specific to BPD. Second, although seed-based connectivity analyses are well suited to address hypothesis driven questions, results are inherently limited to the connections of the a-priori chosen seeds.

This means that differences between BPD patients and controls in neural circuits not associated with one of our seeds might have gone unobserved in the current study.

Data driven methods (including ICA), as used by Wolf et al. (2011) in BPD, do have the potential to look at the data in a more exploratory fashion. Third, BOLD measurements of the amygdala are susceptible to physiological confounds due to its proximity to draining veins. To remove variance associated with these confounding signal sources, we used global signal regression (GSR). Although this method has been proven to be useful in dealing with physiological artifacts and generally increases connection specificity, it is also known to introduce anti-correlations in connectivity analyses (Murphy et al., 2009). Recent research on simulated data demonstrated that GSR could promote connectivity differences between groups due to differences in the underlying noise structure, even when these do not exist (Saad et al., 2012). Therefore, we repeated all analyses without GSR and observed highly similar results, albeit some effects were only found sub-threshold. Importantly, reduced connectivity in the occipital cortex was also observed in a previous RS fMRI study of the DMN in BPD patients that used a different analysis method without GSR (Wolf et al., 2011).

In sum, we observed differences between BPD patients and healthy controls in RSFC of brain regions of high relevance to the disorder. More specific, our findings suggest connectivity changes in brain networks associated with the processing of negative emotions, encoding of salient events and self-referential processing in individuals with BPD compared to healthy individuals. Importantly, our findings corroborate previous resting-state connectivity studies in BPD suggesting an impaired flexibility to switch between large-scale networks during rest. Resting-state fMRI has the potential to map network differences in BPD, and may shed more light on the role of abnormal brain functional connectivity in the pathophysiology of BPD.

Acknowledgements:

A. Krause-Utz was funded by a Ph.D. stipend from the German Research Foundation (SFB636). B.M. Elzinga, and S.A.R.B. Rombouts were funded by VIDI grants from the Netherlands Organization for Scientific Research (NWO) and by the Netherlands Organization for Scientific Research - National Initiative Brain and Cognition (NWO-NIHC, project number 056-25-010). We thank all participants of this study, as well as Claudia Stief and Birgül Sarun for their collaboration in this study.

Declaration of Interest: None.

Supplemental Material

Table S4.1.

Resting-state functional connectivity results without global signal regression:

Region	Hemisphere	Cluster size 2mm voxels	Peak voxel coordinates (MNI)			Z-value
			X	Y	Z	
<u>Amygdala seed</u>						
BPD>HC						
Insula	R	389	34	4	8	4.00*
Orbitofrontal cortex	R		32	12	-22	3.52 *
Putamen	R		28	8	-4	3.04 *
<u>Dorsal ACC seed (I4)</u>						
BPD>HC						
Rostral anterior	R					
(para)cingulate cortex	R		8	40	26	3.67**
			8	52	14	3.42**
HC>BPD						
Posterior cingulate cortex	L		2	-50	24	2.83**
			-14	-58	22	3.27**
<u>Ventral ACC seed (S7)</u>						
BPD>HC						
Medial visual cortex		709	4	-80	4	3.81*

Note: * Z-values are cluster corrected for multiple comparisons ($p<.05$). ** Z-values do not survive cluster correction.

Table S4.2.

DES associations with amygdala connectivity in BPD without global signal regression

Region	Hemisphere	Cluster size 2mm voxels	Peak voxel coordinates (MNI)			Z-value
			X	y	Z	
Positive association						
Dorsolateral prefrontal cortex	R	918	26	48	32	4.33*
Negative association						
Lingual gyrus	R		12	-64	-10	3.23**
Lateral occipital cortex	R		44	-84	-6	4.38**
Fusiform gyrus	R		36	-58	-20	3.1**
Intracalcarine cortex			4	-86	4	3.55**

Note: * Z-values are cluster corrected for multiple comparisons ($p<.05$). ** Z-values do not survive cluster correction.

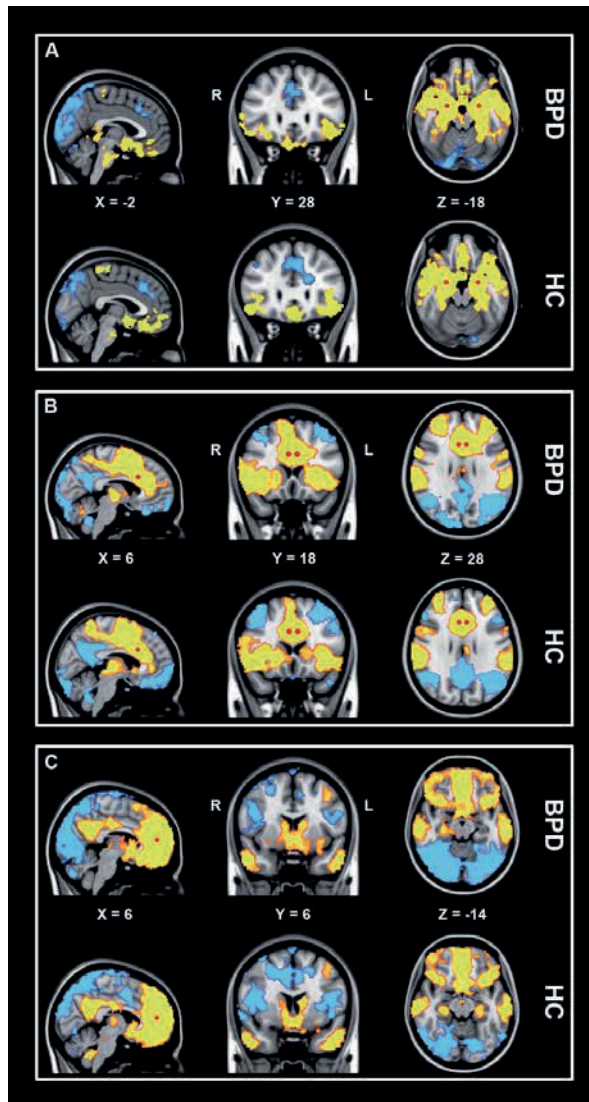


Figure S4. 1. Group main effects demonstrating average RSFC in both groups with each of the three seeds ($Z > 2.3$, $p < .05$; whole brain cluster corrected): A) Amygdala (medial temporal lobe network); B) Dorsal ACC (salience network); C) Ventral ACC (default mode network). Connectivity differences are overlaid on the MNI 2mm standard space template, according to the radiological convention. Positive connectivity is shown in red to yellow, while blue to light blue illustrates negative connectivity. Red spheres mark the locations of the seeds used in the analysis.

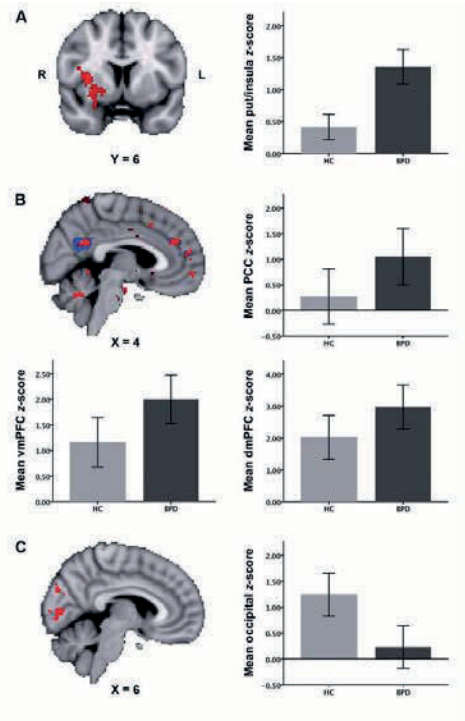


Figure S4.2. Between-group differences in RSFC of each of the three seeds without global signal regression: A) Amygdala (medial temporal lobe network; $p < .05$, cluster corrected); B) Dorsal ACC (salience network; $p < .001$, uncorrected, overlaid on the original result with global signal regression in blue); C) Ventral ACC (default mode network; $p < .05$, cluster corrected). Connectivity differences are overlaid on the MNI 2mm standard space template. Bar graphs plot the mean Z-scores (± 2 SEM) in each group for each of the regions where FC differences are found.

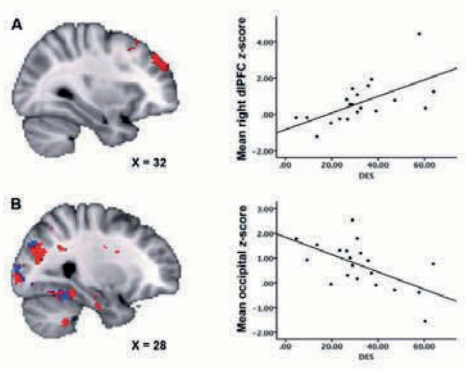


Figure S4.3. Voxel-wise correlations between trait dissociation (DES) and amygdala RSFC without global signal regression in BPD: A) Left amygdala-dIPFC connectivity is positively associated with dissociation ($p < .05$, cluster corrected); B) Left amygdala-occipital cortex FC (including the lingual gyrus, intra-calcarine cortex, and fusiform gyrus) is negatively associated with dissociation ($p < .001$, uncorrected, overlaid on the original result with global signal regression in blue). Results are overlaid on the MNI 2mm standard space template, according to the radiological convention. Scatter plots illustrate the direction of the correlation, with mean Z-scores plotted against DES scores.

Additional information on subgroup analysis:

Since nine BPD patients met criteria for PTSD, we ran an additional post-hoc analysis to assess the effects of comorbidity on FC. Given the small group sizes, this analysis was done on the individual Z-scores within each of the clusters in which we found an effect. Multivariate analysis of variance (MANOVA) was used with Group as between-subjects factor: HC (n=17), BPD without comorbid PTSD (BPD; n=11), and BPD with current PTSD (BPD+PTSD; n=9). Post-hoc *t*-tests were carried out to compare the three groups to each other. The MANOVA revealed a significant group effect ($p < .001$). Between-subjects effects were found for each of the five clusters of the whole-brain analysis (all p 's $< .006$). Post-hoc tests revealed significant differences between BPD and HC for each cluster (p 's $< .01$) as well as between BPD+PTSD and HC (p 's $< .05$), except for ventral ACC connectivity with the occipital cortex ($p = .10$). No differences were found between the two BPD subgroups (p 's $> .5$). The association between DES scores and left amygdala connectivity with the DLPFC and occipital cortex was observed in both BPD subgroups as well, while DES scores did not differ between the two groups ($p = .33$).

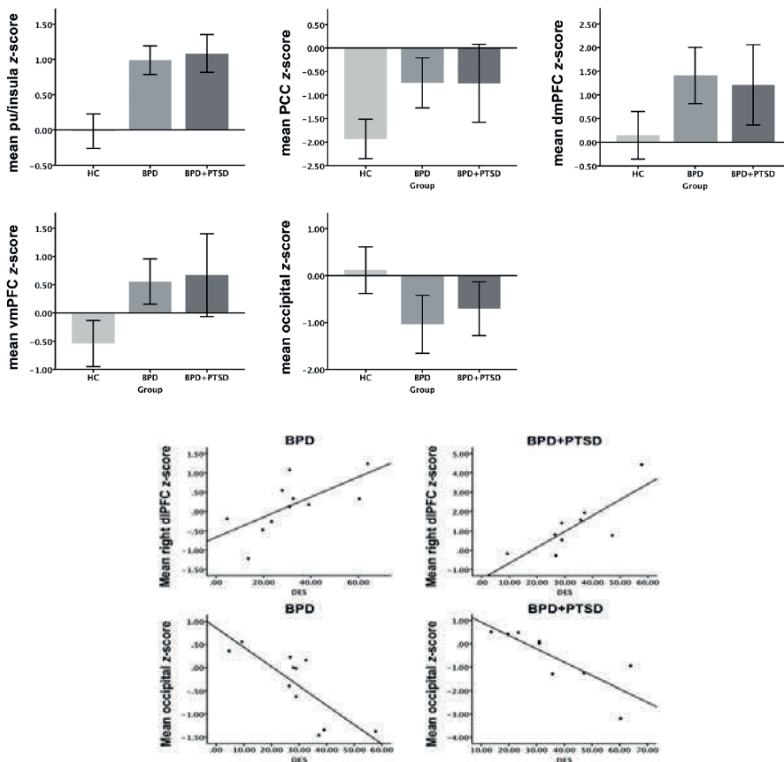


Figure S4.4. Subgroup analysis for HC, BPD patients with comorbid PTSD (BPD+PTSD), and patients without PTSD (BPD). Bar graphs plotting mean Z-scores (± 2 SEM) for each cluster found in the main analysis.